



OPEN

Estrogen associates with female predominance in Xp11.2 translocation renal cell carcinoma

Yanwen Lu¹, Yiqi Zhu¹, Wenliang Ma¹, Ning Liu¹, Xiang Dong¹, Qiancheng Shi¹, Fei Yu², Hongqian Guo¹, Dongmei Li^{3,4} & Weidong Gan¹✉

Based on the epidemiological characteristics of susceptibility and age selectivity for women in Xp11.2 translocation renal cell carcinoma (Xp11.2 tRCC), we inferred that estrogen was to be blamed. Rad54 like 2 (*Rad54l2*) which might be one of key effector proteins of DNA damage mediated by estrogen was downregulated in numerous cancers, however, its role in epidemiological characteristics of Xp11.2 tRCC was needed to further study. We reviewed 1005 Xp11.2 tRCC cases and collected estrogen data and then compared the onset time of Xp11.2 tRCC cases in female with estrogen changing trend.

An RNA-sequencing was performed in estrogen treated HK-2 cells and subsequently bioinformatic analysis was applied based on the Cancer Genome Atlas (TCGA) and GEO database. The male-to-female ratio of Xp11.2 tRCC was 1:1.4 and the median age of onset was 29.7 years old. The onset trend of female was similar to estrogen physiological rhythm ($r = 0.67$, $p < 0.01$). In Xp11.2 tRCC and HK-2 cells after estrogen treatment, *Rad54l2* was downregulated, and GSEA showed that pathways significantly enriched in DNA damage repair and cancer related clusters after estrogen treated, as well as GO and KEGG analysis. Downregulation of *Rad54l2* was in numerous cancers, including renal cell carcinoma (RCC), in which *Rad54l2* expression was significantly decreased in male, age over 60 years old, T2&T3&T4 stages, pathologic SII&SIII&SIV stages as well as histologic G3&G4 grades, and cox regression analysis proved that *Rad54l2* expression was a risk factor for overall survival, disease-specific survival and progression-free interval in univariate analysis. There existed female predominance in Xp11.2 tRCC and *Rad54l2* might play vital role in estrogen mediating female predominance in Xp11.2 tRCC.

Xp11.2 translocation renal cell carcinoma (Xp11.2 tRCC) was firstly defined as a distinctive renal cell carcinoma (RCC) entity in 2004¹ and then reclassified into microphthalmia (MiT) family tRCC in 2016². This category of RCC is caused by breakage of the transcription factor enhancer 3 (*TFE3*) gene on X-chromosome and then balanced translocation with partner genes, such as *ASPL*, *PRCC*, *SFPQ*, *NonO* and *CLTC*³⁻¹⁰.

Xp11.2 tRCC was firstly reported in a two-year-old child¹¹. Recent literatures showed that Xp11.2 tRCC occurred mostly in young people¹² and the median age of onset is 29 years old¹³. However, in non-Xp11.2 tRCC, the median age is in the sixth and seventh decades¹⁴. A meta-analysis had revealed that the incidence of female is higher than that of male¹⁵, which is similar to the previous report by Cheng et al.¹⁶. In contrast, large-scale epidemiological investigation show that RCC is more common in male regardless of pathological type with a male-to-female ratio of 2:1¹⁷. Therefore, female predominance in childbearing period may be a noteworthy feature of Xp11.2 tRCC according to the age and gender data.

The gender disparity in RCC had been shown to be associated with sex steroids^{18,19}. Preceding literature had also reported that estrogen could increase risk of topoisomerase II β -mediated *TFE3* breaks to initiate Xp11.2 tRCC²⁰. This epidemiological feature may suggest that estrogen is a risk factor of Xp11.2 tRCC.

Moreover, androgen and androgen receptor could facilitate Xp11.2 tRCC progression²¹. Estrogen influenced the DNA damage response (DDR) and DNA repair through the regulation of key effector proteins, such as ATR,

¹Department of Urology, Nanjing Drum Tower Hospital, The Affiliated Hospital of Nanjing University Medical School, No. 321 Zhongshan Road, Nanjing 210008, Jiangsu, People's Republic of China. ²Department of Laboratory Medicine, Nanjing Children's Hospital, The Affiliated Hospital of Nanjing Medical University, Nanjing, Jiangsu, People's Republic of China. ³Immunology and Reproduction Biology Laboratory and State Key Laboratory of Analytical Chemistry for Life Science, Medical School, Nanjing University, Nanjing, Jiangsu, People's Republic of China. ⁴Jiangsu Key Laboratory of Molecular Medicine, Nanjing University, Nanjing, Jiangsu, People's Republic of China. ✉email: gwd@nju.edu.cn

ATRX, Rad51, Rad54b²². Rad54 like 2 (*Rad54l2*), a paralog of DNA repair and recombination protein *Rad54b*, participated in super-helical torsion within linear DNA fragments in an ATP-dependent manner²³. It was widely involved in replication and DNA repair²⁴, previous study also reported that Rad54l2 was downregulated after radiotherapy, indicating impaired DNA repair capacity²⁵. However, no systemic investigation into its role was carried out in the induction of Xp11.2 tRCC.

In this study, firstly, we demonstrated female predominance in Xp11.2 tRCC, and the onset trend of female was similar to estrogen physiological rhythm. Then, we explored the expression of Rad54l2 in Xp11.2 tRCC and HK-2 cells after estrogen treatment with RNA-sequencing and bioinformatic analysis to study the role of estrogen in Xp11.2 tRCC. Finally, we investigated Rad54l2 expression in many malignant tumors, including RCC and evaluated its role in RCC through bioinformatic analysis. These findings may offer a novel perspective to explain that estrogen was to be blamed for the female predominance of Xp11.2 tRCC.

We present the following article in accordance with the MDAR reporting checklist.

Materials and methods

Literature search and study selection. We performed a nonsystematic review in Cochrane, DARE, MEDLINE, EMBASE and PubMed using key words “Xp11.2 translocation”, “*TFE3*” and “renal cell carcinoma”. Since Xp11.2 tRCC was first reported in 1986, articles published from 1 January 1986 to 31 December 2020 was selected. All listed articles were reviewed carefully, in case of some cases repeated and left out. The diagnosis of Xp11.2 tRCC was based on: (1) strong TFE3 nuclear positivity by immunohistochemical staining; (2) Positive results in TFE3 break-apart FISH; (3) Confirmation by RNA-sequencing or karyotyping.

Estrogen data collection. We collected estrogen data from Affiliated Nanjing Drum Tower Hospital of Medical School of Nanjing University and Nanjing Children’s Hospital. The inclusion criteria were as followed: (1) healthy people; (2) Estrogen level was not influenced. Finally, estrogen data from 1800 patients were enrolled in this study. The serum concentration of estrogen from the 1800 samples were tested by chemiluminescent immunoassay. The study protocol was approved by the ethics committee of Affiliated Nanjing Drum Tower Hospital of Medical School of Nanjing University and Nanjing Children’s Hospital and conformed to the principles of the Declaration of Helsinki. Data collection was approved by the institutional review board and performed in accordance with the ethical standards established by Nanjing Drum Tower Hospital of Medical School of Nanjing University and Nanjing Children’s Hospital. Written informed consent was obtained from all included samples before the clinical investigations were performed.

RNA-sequencing. HK-2 cells treated with 10 nmol/L estrogen for 24 h were harvested, then total RNA was isolated by using TRIzol reagent (Vazyme, R401) following the manufacturer’s procedure. The RNA amount and purity of each sample was quantified with RIN number > 7.0, OD₂₆₀/OD₂₈₀ > 1.8, total RNA > 1 µg. At last, we performed the 2 × 150 bp paired-end sequencing (PE150) on an illumina Novaseq™ 6000 (LC-Bio Technology CO., Ltd., Hangzhou, China) following the vendor’s recommended protocol.

Bioinformatics analysis of RNA-seq. Fastp software (<https://github.com/OpenGene/fastp>) were used to make quality control for raw data. HISAT2 (<https://ccb.jhu.edu/software/hisat2>) were used to map reads to the reference genome of Homo sapiens GRCh38. We used StringTie (<https://ccb.jhu.edu/software/stringtie>) with default parameters to assemble the mapped reads. After the final transcriptome was generated, StringTie was used to estimate the expression levels of all transcripts and mRNAs by calculating FPKM. We denied the differentially expressed mRNAs with fold change > 2 or fold change < 0.5 and with parametric F-test comparing nested linear models (p value < 0.05) by R package edgeR (<https://bioconductor.org/packages/release/bioc/html/edgeR.html>). Gene set enrichment analysis (GSEA) was operated according to the given gene set from the Molecular Signatures Database (MSigDB) (<http://software.broadinstitute.org/gsea/msigdb>). Gene Ontology (GO) and Kyoto Encyclopedia of Genes and Genomes (KEGG) were analyzed by R package “clusterProfiler”.

Cell culture and reagent. The cell line HK-2, 786-O was purchased from ATCC. UOK109 and UOK120 were a gift of Marston Linhan from NIH. All cells were maintained in 90% Dulbecco’s Modified Eagle Medium (Gibco, 10569010) supplemented with 10% fetal bovine serum (Gibco, 16140063) and 1% penicillin/streptomycin (Invitrogen, 15070063) in 5% CO₂ at 37 °C. E2 (Sigma-Aldrich, E8875) was dissolved in DMSO (Sigma-Aldrich, D2650).

RNA isolation and quantitative real-time PCR. TRIzol extraction reagent (Vazyme, R401) was used to isolate total RNA which was then reverse-transcribed using a Reverse Transcriptase master mixing kit (Vazyme, R201) according to the manufacturer’s procedure. Primers (18s rRNA forward primer: CAGCCACCCGAGATT GAGCA, 18s rRNA reverse primer: TAGTAGCGACGGCGGTGTG; Rad54l2 forward primer: AGGAGTGTG ACAGGGATGATG; Rad54l2 reverse primer: TCCTCGGAGGCTAGTTCTTG; ER-α forward primer: AGA TCTTCGACATGCTGCTGGCTA, ER-α reverse primer: AGACTTCAGGGTGTGACAGAAA; ER-β forward primer: TGGGCACCTTCTCCTTTAGTGGT, ER-β reverse primer: TCTTGCTTCACACCAGGGACT CTT) were synthesized by Tsingke Biological Technology. PCR amplifications were operated by using SYBR Green (Vazyme, Q711) and ABI ViiA7 System (Applied Biosystems). Relative expression of target gene was calculated by the comparative 2^{-(ΔΔCt)} method normalizing on 18S rRNA.

Data mining the GEO database. Rad54l2 mRNA expression and clinical data were from GEO database (GSE167573) and (GSE150474), in GSE167573, there were 63 Xp11.2 tRCC cases and 14 normal cases. 12 Xp11.2 tRCC cases and 7 normal cases were included in GSE150474. Ethical approval was not required, as all are open to the public. High-throughput sequencing and clinical data were analyzed using R software (version 3.6.3).

Statistical analysis. According to the distribution of demographic characteristics, all cases were grouped by a 5-year interval. Then we calculated the number of cases and average estrogen levels in each group. Taking age as abscissa, the number of male and female cases and the variation trend of estrogen with age were plotted respectively. Unpaired t-test was used to analyze the significance of cases among different age groups by GraphPad Prism software version 8.0 (GraphPad Software, San Diego, CA). The correlation analysis was used to evaluate the relationship between female cases and physiological rhythm of estrogen levels by Origin 2018 (OriginLab, Northampton, Massachusetts, USA). Student's t-test was used to assess differences in Rad54l2 mRNA expression between different groups. Kaplan–Meier curve was performed to evaluate the survival status using the log-rank test. Receiver operator characteristic (ROC) curve were drawn to assess the prognostic value of Rad54l2. Univariate and multivariate analyses were performed using a Cox proportional hazard regression model. A two-tailed p-value of <0.05 was considered to be statistically significant.

Results

Similar trends between the onset trend of female and estrogen physiological rhythm in Xp11.2 tRCC. After excluding the unqualified literature, a total of 169 articles fulfilled the inclusion criteria. Of 1005 enrolled Xp11.2 tRCC patients, 417 were men and 584 were women (male-to-female ratio = 1:1.4). 295 male cases and 383 female cases with exact age of onset from initially 1005 cases were selected, with male-to-female ratio = 1:1.3. Overall, the age of onset ranged from 1 to 85 years old with median age approximately 29.7 years old (Fig. 1A,B). There were 124 cases under 16 years old, accounting for 18.29%. 382 cases were at the age of 16–45 during child-bearing period, which made up of 56.53%. After 45 years old, there were 172 cases with the proportion of 25.37% (Table 1). For trend analysis, the difference in sex ratio can be divided into three stages and the results were shown in Table 1. From childhood to adolescence, the number of Xp11.2 tRCC cases was consistently raised. Before the age of 16, the incidence of Xp11.2 tRCC in women was similar to that in men ($p > 0.05$) with the male-to-female ratio of 1.3:1. Between 16 to 45 years old, the number of male cases remained stable, however, the quantity of female cases increased sharply, with a peak value in age group of 16–20 years old. The number of female cases was more than that of male significantly ($p < 0.05$), with male-to-female ratio = 1:1.45. After 45 years old, especially after 66 years old, the quantity of male cases was approximately equal to female cases ($p > 0.05$) (Fig. 1C). Estrogen levels rose from childhood and reached to a peak value in age group of 21–25 years old, then remained at a high level until the age of 45. This result was consistent with the physiological changes of estrogen levels in female. In addition, there was a significant correlation ($r = 0.67$, $p < 0.01$) between the number of female cases and the changes of estrogen (Fig. 1D).

Rad54l2 was downregulated in HK-2 cell treated with estrogen and Xp11.2 tRCC. Previous study in our center demonstrated that estrogen induced *TFE3* breakage dependent on ER in the renal tubular epithelial cell HK-2 cell²⁰, however, which molecule mediated this process was uncovered. Therefore, an RNA-sequencing which after HK-2 cell was treated with estrogen 24 h at a concentration of 10 nM was conducted. It was verified that Rad54l2 was significantly downregulation after estrogen treatment among DNA repair related genes (Fig. 2A), whereafter qRT-PCR further confirmed this result (Fig. 2B). It was suggested that some pathways were enriched, including positive regulation of response to DNA damage stimulus and regulation of response to DNA damage stimulus in GO and DNA replication in KEGG analysis (Fig. 2C,D). In addition, according to GSEA, Rad54l2-associated differentially expressed genes were enriched in DNA damage repair related clusters, involved in base excision repair, mismatch repair, nucleotide excision repair and UV response down (Fig. 2E–H). Results from GEO database (GSE167573) and (GSE150474) observed that Rad54l2 was also dramatically downregulation when compared with normal tissue in Xp11.2 tRCC (Fig. 2I,J), as well as, GSEA enriched significantly in UV response down cluster and DNA repair pathway (Fig. 2K,L). GSEA analysis found that after HK-2 cell treatment with estrogen, Rad54l2-associated differentially expressed genes were also enriched in cancer pathway, including small cell lung cancer, pancreatic cancer, colorectal cancer, non-small cell lung cancer, glioma, acute myeloid leukemia, chronic myeloid leukemia, basal cell carcinoma, melanogenesis, melanoma (Fig. 3A–K), as well as for RCC (Fig. 3L), in addition, endometrial cancer and prostate cancer were also significantly enriched (Fig. 3M,N), which partial caused by hormone in oncogenesis.

Expression profiles of Rad54l2 in numerous cancers. We utilized the cancer genome atlas (TCGA) online database to determine the mRNA of Rad54l2. As shown in (Fig. 4A), among 38 cancer types, the Rad54l2 was significantly low-expressed in 10 cancers, except for stomach adenocarcinoma. Moreover, Rad54l2 expression was much lower in KRIC tumors than in normal tissues ($P < 0.001$, Fig. 4B). Interestingly, expression of Rad54l2 in skin cutaneous melanoma metastasis is higher than that in primary sites.

Association of Rad54l2 expression and clinicopathological characteristics in RCC patients. Clinicopathological characteristics of RCC with differentially expressed Rad54l2 were collected, as shown in Table 2. Patients in Rad54l2-low group presented a higher percent of male sex, older age, much more severe clinical T stage, worse pathologic stage and poorer histologic grade when compared to the Rad54l2-high group. Nevertheless, clinical N stage and M stage were without significant difference between two groups.

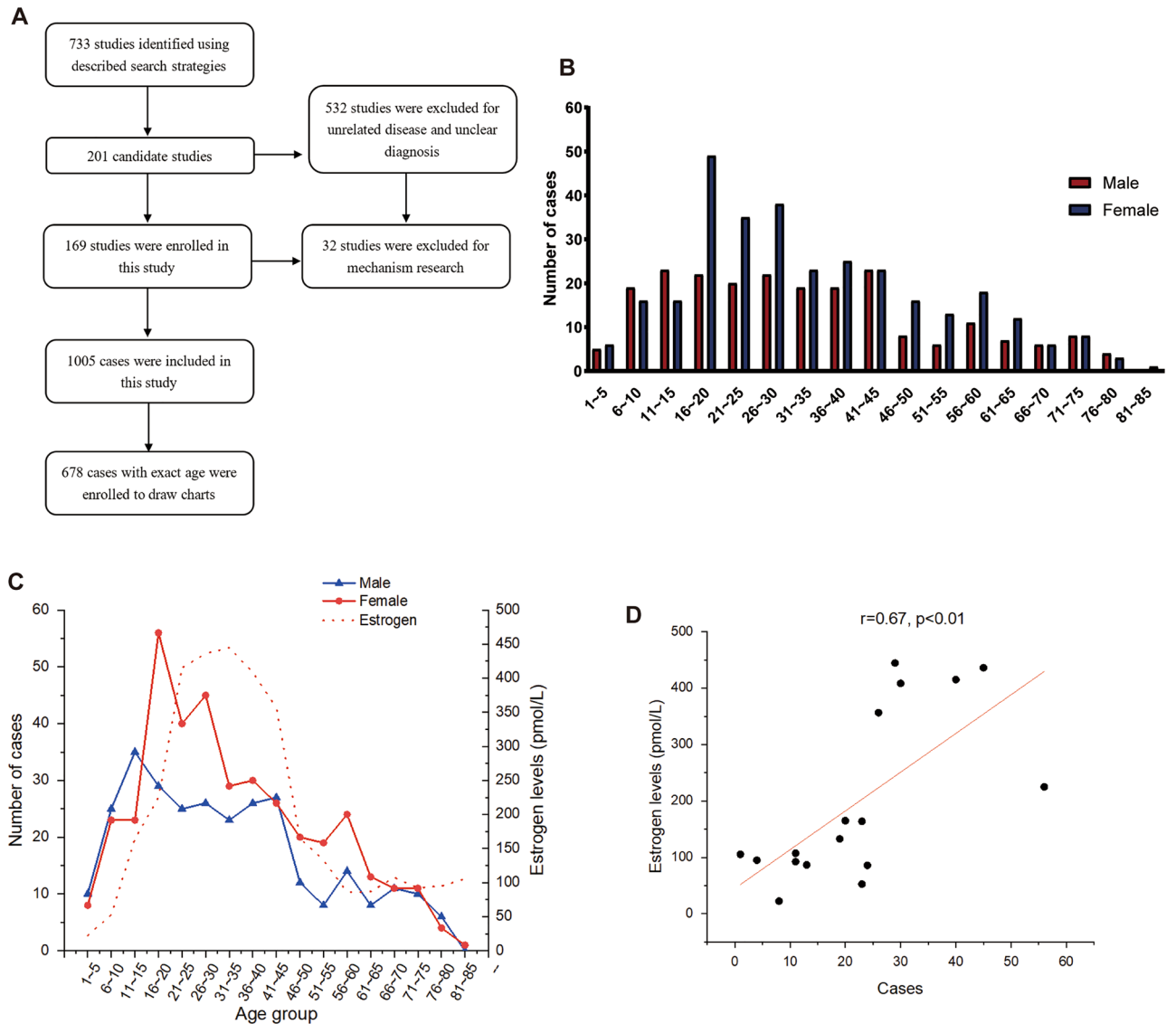


Figure 1. Similar trends between the onset trend of female and estrogen physiological rhythm in Xp11.2 tRCC. **(A)** Flow diagram of study selection. **(B)** The gender distribution in different age groups. **(C)** The trend of the onset time of Xp11.2 tRCC cases in female and estrogen levels. **(D)** Correlation analysis of the trends of female cases and estrogen changing trend with age. n.s.: $p \geq 0.05$; * $p < 0.05$; ** $p < 0.01$; *** $p < 0.001$; **** $p < 0.0001$.

Furthermore, we analyzed Rad54l2 expression in patients with different clinicopathological characteristics. As shown in (Fig. 5A–E), Rad54l2 expression was significantly decreased in male sex, age over 60 years old, T stages T2, T3 and T4, pathologic stages Stage II, Stage III and Stage IV, histologic grade Grade3 and Grade 4.

Predictive value of Rad54l2 for RCC diagnosis and prognosis. ROC curve analysis was used to analyze the power of Rad54l2 in the differential diagnosis of RCC patients. Based on the area under curve (AUC) being 0.808, Rad54l2 showed significant high sensitivity and specificity for RCC diagnosis (Fig. 6A). Subsequently, we utilized K-M analysis to demonstrate the role of Rad54l2 in RCC prognosis. It is suggested that overall survival (OS), disease-specific survival (DSS) and progression-free interval (PFI) for low-Rad54l2 group were all significantly poorer than high-Rad54l2 group (Fig. 6B–D). As well as, we conducted a cox regression analysis to further confirm the forecast value of Rad54l2 on prognosis. As shown in Table 3, Rad54l2 expression was a risk factor for OS, DSS and PFI. A prognostic nomogram was drawn by using all the statistically significant prognostic factors in each cox regression analysis. The nomogram consisted of T stages, M stages and Rad54l2 expression (Fig. 6E–G). Then, we drawn a calibration curve was to verify the efficiency of each nomogram. All the curves shown dramatically favorable prediction of the nomogram for the 1-, 3-, and 5-year clinical outcomes (Fig. 6H–J).

Age group	Males (n = 295)	Females (n = 383)	p value
0–15	10	8	> 0.05
	25	23	
	35	23	
16–45	29	56	< 0.05
	25	40	
	26	45	
	23	29	
	26	30	
	27	26	
46–85	12	20	> 0.05
	8	19	
	14	24	
	8	13	
	11	11	
	10	11	
	6	4	
	0	1	

Table 1. Gender disparity between male and female in different age groups.

Discussion

In the past few decades, sex hormones have been shown to have a certain effect on the development and progression of RCC^{26,27}. However, the effect of sex hormone in Xp11.2 tRCCs was not evaluated. The present study which conducted with more than 1000 Xp11.2 tRCC cases was the largest case collection to date. The results showed that the overall male-to-female ratio of Xp11.2 tRCC was 1:1.4, which is different from the male-to-female ratio of incidence in conventional RCC. Interestingly, this female advantage mainly occurred during 16–45 years old, when estrogen was maintained at a high level in women. The starting and ending time of female advantage of incidence in Xp11.2 tRCC corresponded to the estrogen level in adolescence and menopause period, respectively, indicating estrogen physiological rhythm was correlated to female predominance during child-bearing period.

We observed that Rad54l2 was downregulation in HK-2 cells after estrogen treatment and Xp11.2 tRCC. In addition, GSEA showed that pathways significantly enriched in DNA damage repair and cancer related clusters after estrogen treated. GO and KEGG analysis also got similar results. Rad54l2 expression in RCC, was significantly decreased in male, age over 60 years old, T2&T3&T4 stages, pathologic SII&SIII&SIV stages as well as histologic G3&G4 grades, and cox regression analysis proved that Rad54l2 expression was a risk factor for OS, DSS and PFI in univariate analysis.

Defects in DNA repair pathway are key steps for tumorigenesis, incorrectly repaired DNA breaks could result in chromosome instability and progression to cancer²⁸. Rad54l2 binds to DNA and mononucleosomes and involves in chromatin remodeling, DNA excision repair and homologous recombination²⁹, whose reduction would result in impaired DNA repair, thus chromosome translocation. Previous study has demonstrated that irradiation also downregulates Rad54l2, accompanied by γ H2A.X increment, which indicates DNA damage occurred²⁵.

It is suggested that estrogen is a complete carcinogen, being capable of tumor formation by suppressing DNA repair to allow the accumulation of genomic change conducive to tumorigenesis²². Estrogen receptors (ERs) are discovered in both normal kidney tissue and kidney cancer³⁰, indicating estrogen works in kidney cancer. It is proved that ER α could regulate negatively ATM and ATR which are key initiators of DDR³¹. In addition, ER α could also impact on DNA repair through interacting directly with various DNA repair proteins, including FEN1, MPG, APE1, and TDG of the BER pathway, NHEJ repair proteins Ku70 as well as Ku86, MSH2 of the MMR pathway³².

Xp11.2 tRCC is characterized by *TFE3* gene breakage on X chromosome. For tumor involving X chromosome, the number advantage of X chromosome is a probable cause of female predominance³³. However, synovial sarcoma with balanced translocation t(X;18), which pathogenesis is similar to Xp11.2 tRCC, showed male predominance³⁴. In addition, alveolar soft part sarcoma which involves with unbalanced translocation of *TFE3* showed similar incidence rate between male and female³⁵. These results indicated that female predominance did not always appear in cancers involving the X chromosome. Therefore, the number of X chromosome could not completely explain the sex difference in morbidity.

It is reported that prior exposure to TOP2 poison may induce DNA double-strand breaks (DSBs) and thus result in Xp11.2 tRCC formation^{36,37}. Many animal models also demonstrated that estrogen can induce microsatellite DNA alterations and DNA single-strand breaks in Syrian hamsters and led to kidney cancer^{26,38–41}, which is similar to the impact of estrogen in breast cancer^{42,43}. Accumulated evidences support that estrogen metabolites, 2-hydroxy-estrogen (2-OHE2) and 16 α -hydroxyoestrone (16 α -OHE1) generate reactive oxygen species^{44–46}, resulting in DNA breakage. Among a number of diseases related to estrogen metabolism, many show female predominance similarity with Xp11.2 tRCC. For instance, pulmonary arterial hypertension (PAH) has a similar

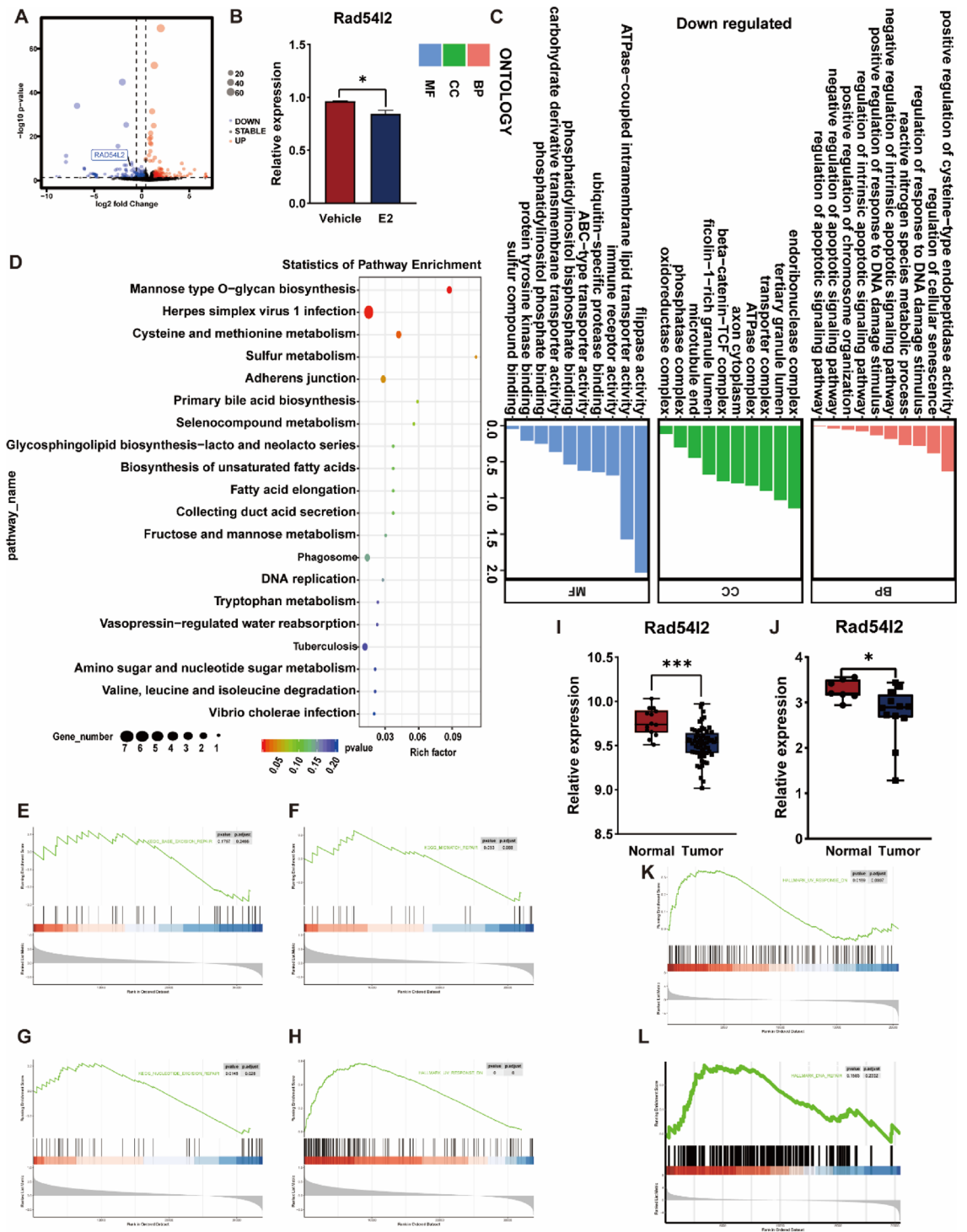


Figure 2. Rad54l2 was downregulated in HK-2 treated with estrogen and Xp11.2 tRCC. (A) RNA-sequencing found that Rad54l2 was downregulated after estrogen treatment. (B) qRT-PCR further confirmed this result. (C,D) GO and KEGG analysis enriched in DNA damage repair related clusters in RNA-sequencing. (E–H) GSEA enrichment analysis in DNA damage repair related clusters in RNA-sequencing. (I,J) Rad54l2 mRNA was downregulated in Xp11.2 tRCC. Data from (GSE167573) and (GSE150474) respectively. (K,L) GSEA analysis enriched in UV response down in Xp11.2 tRCC. Data from (GSE167573).

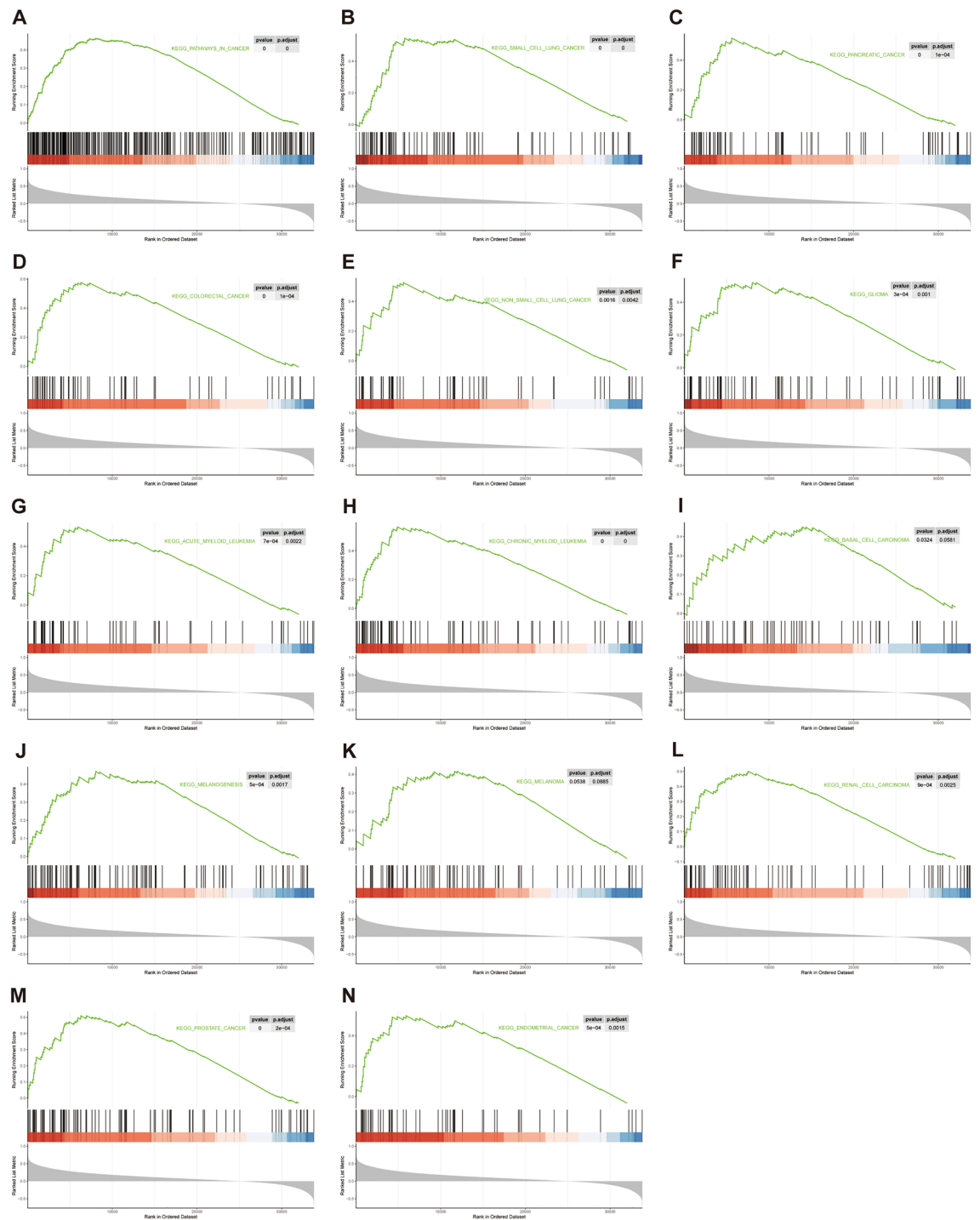


Figure 3. Cancer related clusters were enriched in GSEA analysis. Pathways in (A) cancer, (B) small cell lung cancer, (C) pancreatic cancer, (D) colorectal cancer, (E) non-small cell lung cancer, (F) glioma, (G) acute myeloid leukemia, (H) chronic myeloid leukemia, (I) basal cell carcinoma, (J) melanogenesis, (K) melanoma as well as for (L) renal cell carcinoma, in addition, (M) endometrial cancer and (N) prostate cancer were significantly enriched as well.

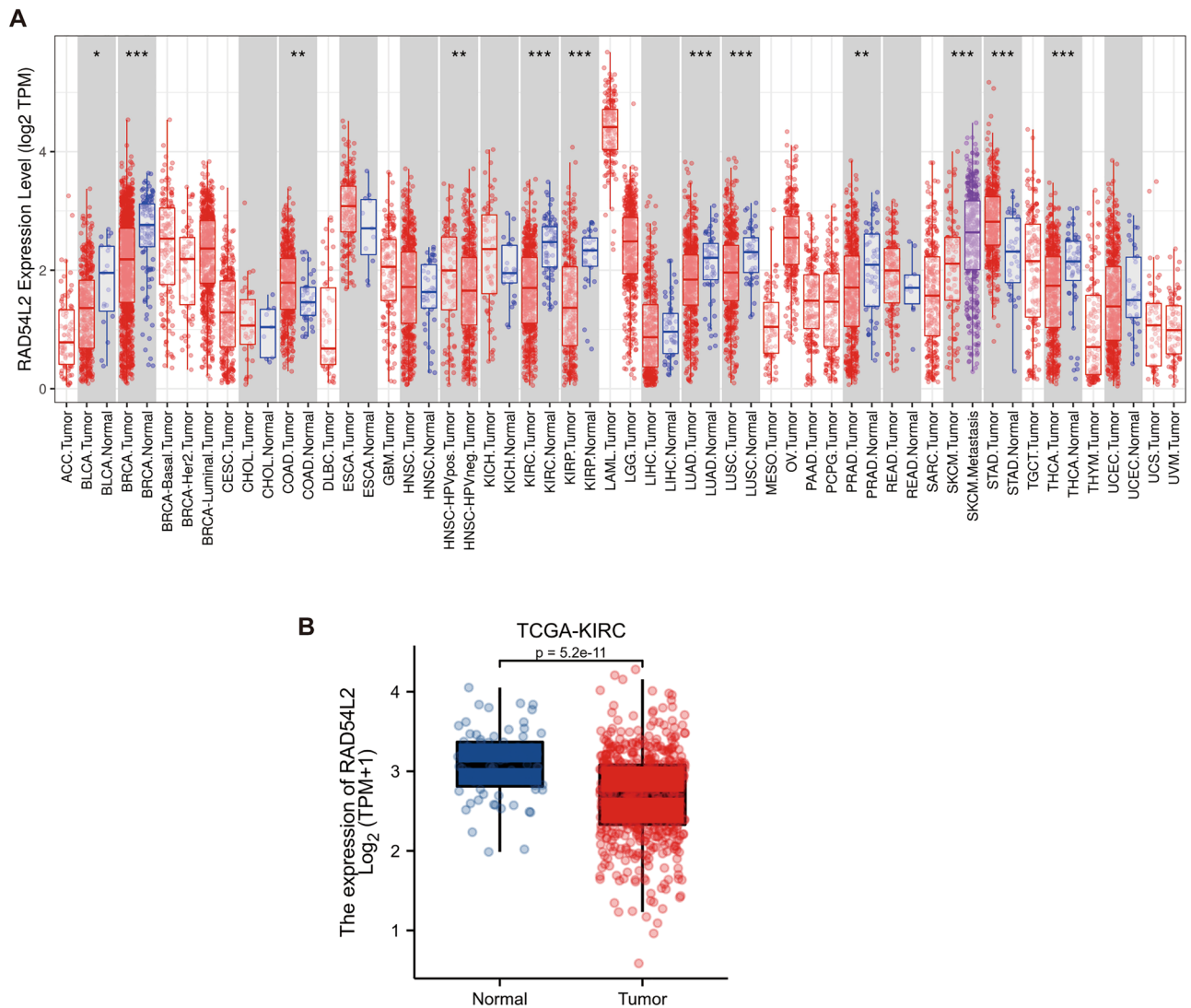


Figure 4. Expression profiles of Rad54l2 mRNA in numerous cancers. **(A)** Rad54l2 expression in a plenty of cancers between tumor and tumor-adjacent tissue. **(B)** Rad54l2 is higher than pericarcinous tissue in RCC.

incidence trend with Xp11.2 tRCC, with male-to-female ratio 1:1.7, mean age 36.4 years old⁴⁷. It is suggested that the ratio of 2-OHE2/16 α -OHE1 can influence PAH attack rate^{47–49}. In addition, the increase of Estrogen-DNA adduct makes female more susceptible to Fuchs endothelial corneal dystrophy and lung cancer^{50,51}.

Our results should be interpreted cautiously. For the rarity of Xp11.2 tRCC, case reports were also included and our search items were likely to be inadequate for all cases included, in addition, clinicopathological data form RCC were applied to confirm the role of Rad54l2 in diagnostic and prognosis value, which might seem to be unreasonable. Considering the low incidence of Xp11.2 tRCC and the lack of effective preoperative diagnostic methods as well as estrogen data from Xp11.2 tRCC were scarcely possible to obtain, so we conducted the analyses using estrogen data from patients with estrogen levels uninfluenced. We were inclined to believe that estrogen through Rad54l2 caused this female predominance of Xp11.2 tRCC, but this hypothesis should be proven by further studies.

In conclusion, this population-based study gives a new insight to the sex differences in Xp11.2 tRCC. The change trend of estrogen during different periods is in accordance with the curve of the onset age in female. Rad54l2 was also shown diagnostic and prognosis value for RCC. The downregulated Rad54l2 in Xp11.2 tRCC and HK-2 with estrogen treatment might be a key factor for estrogen mediating chromosome translocation. These findings suggest that estrogen is a potential pathogenic factor of Xp11.2 tRCC although more molecular evidences are needed.

Characteristic	Low expression of RAD54L2	High expression of RAD54L2	p
n	265	265	
Gender, n (%)			0.005
Female	77 (14.5%)	109 (20.6%)	
Male	188 (35.5%)	156 (29.4%)	
Age, n (%)			0.019
≤ 60	118 (22.3%)	146 (27.5%)	
> 60	147 (27.7%)	119 (22.5%)	
T stage, n (%)			0.020
T1	118 (22.3%)	153 (28.9%)	
T2	39 (7.4%)	30 (5.7%)	
T3	103 (19.4%)	76 (14.3%)	
T4	5 (0.9%)	6 (1.1%)	
N stage, n (%)			1.000
N0	115 (45.1%)	124 (48.6%)	
N1	8 (3.1%)	8 (3.1%)	
M stage, n (%)			0.711
M0	208 (41.8%)	212 (42.6%)	
M1	41 (8.2%)	37 (7.4%)	
Pathologic stage, n (%)			0.011
Stage I	115 (21.8%)	150 (28.5%)	
Stage II	30 (5.7%)	27 (5.1%)	
Stage III	75 (14.2%)	48 (9.1%)	
Stage IV	44 (8.3%)	38 (7.2%)	
Histologic grade, n (%)			0.004
G1	2 (0.4%)	12 (2.3%)	
G2	103 (19.7%)	124 (23.8%)	
G3	113 (21.6%)	93 (17.8%)	
G4	44 (8.4%)	31 (5.9%)	

Table 2. Clinicopathological characteristics of RCC patients with differential Rad54l2 expression. RCC renal cell carcinoma.

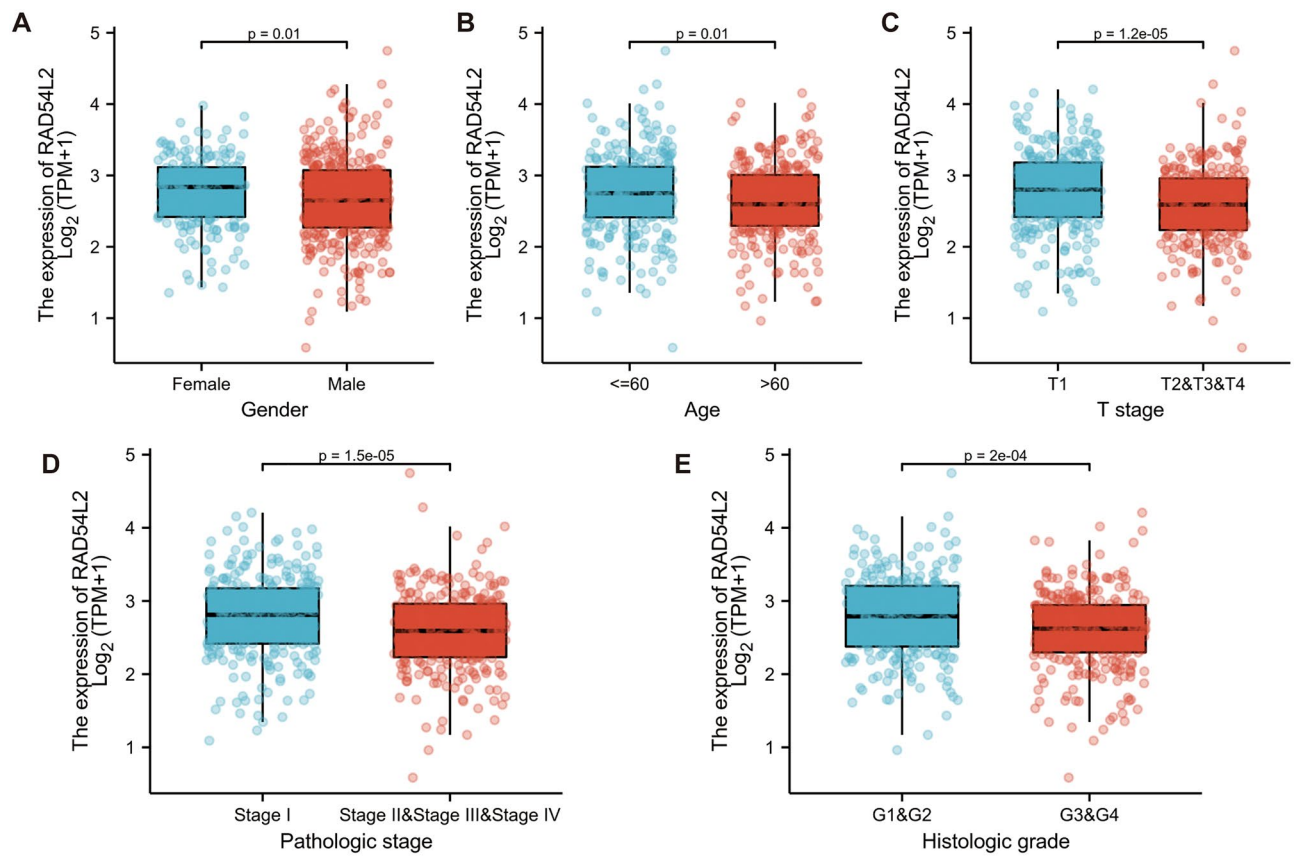


Figure 5. Association of Rad54l2 Expression and Clinicopathological Characteristics in RCC Patients. The association of Rad54l2 Expression with (A) Gender, (B) Age, (C) T stage, (D) Pathologic stage, (E) Histologic grade was analyzed.

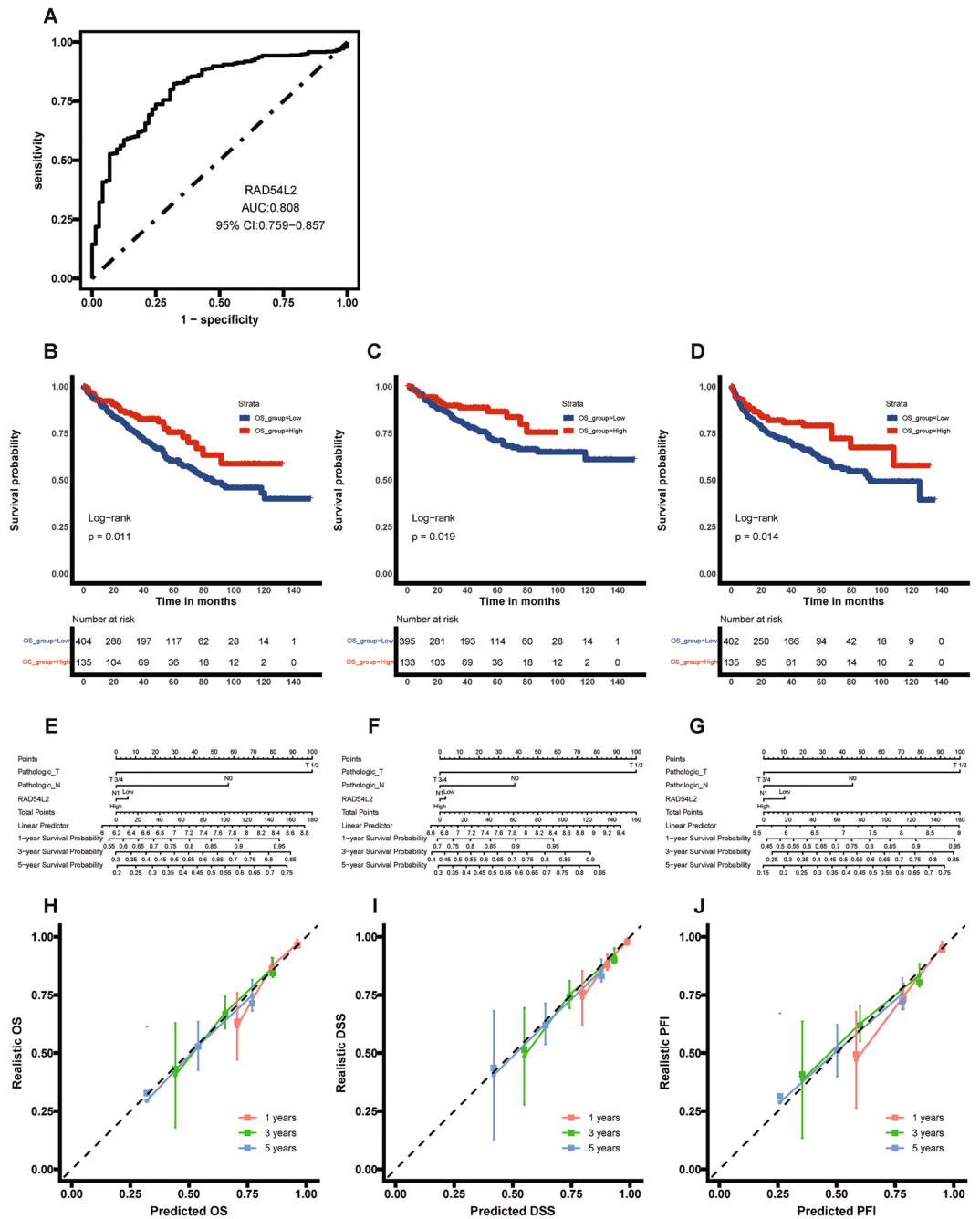


Figure 6. Predictive value of Rad54l2 for RCC diagnosis and prognosis. **(A)** The value of Rad54l2 for RCC diagnosis was analyzed by Receiver operating characteristic (ROC) curve. **(B–D)** K–M curve for OS, DSS and PFI between Rad54l2-high and Rad54l2-low groups. **(E–G)** Rad54l2-based risk scoring models for 1-, 3-, and 5-year OS, DSS and PFI were constructed in nomograms. **(H–J)** Calibration curves were drawn to test the efficiency of the corresponding nomograms for OS, DSS and PFI.

Characteristics	HR for overall survival	HR for progression-free interval	HE for disease-specific survival
Age (> 60 vs. ≤ 60)	1.80****	1.33	1.40
Sex (male vs. female)	0.93	1.52*	1.22
Stage (stage III/IV vs. stage I/II)	3.95****	6.82****	9.83****
Histological grade (grade III/IV vs. stage I/II)	2.70****	3.65****	4.79****
T stage (T3–T4 vs. T1–T2)	3.23****	4.52****	5.54****
N stage (N1–N2 vs. N0)	3.45****	3.68****	3.85****
M stage (M1 vs. M0)	4.39****	8.97****	9.11****
Smoker (yes vs. no)	0.79	1.06	1.22
RAD54L2 (high vs. low)	0.60*	0.60*	0.54*

Table 3. Cox regression analysis for clinical outcomes in RCC patients. HR hazard ratio; *p < 0.05; ****p < 0.0001.

Data availability

The RNA-sequencing data analyzed in this study are not publicly available but can be obtained from the corresponding author.

Received: 15 November 2022; Accepted: 12 April 2023

Published online: 15 April 2023

References

- Lopez-Beltran, A. *et al.* 2004 WHO classification of the renal tumors of the adults. *Eur. Urol.* **49**(5), 798–805 (2006).
- Moch, H. *et al.* The 2016 WHO classification of tumours of the urinary system and male genital organs-Part A: Renal, penile, and testicular tumours. *Eur. Urol.* **70**(1), 93–105 (2016).
- Argani, P. *et al.* Primary renal neoplasms with the ASPL-*TFE3* gene fusion of alveolar soft part sarcoma: A distinctive tumor entity previously included among renal cell carcinomas of children and adolescents. *Am. J. Pathol.* **159**(1), 179–192 (2001).
- Argani, P. *et al.* PRCC-*TFE3* renal carcinomas: Morphologic, immunohistochemical, ultrastructural, and molecular analysis of an entity associated with the t(X;1)(p11.2;q21). *Am. J. Surg. Pathol.* **26**(12), 1553–1566 (2002).
- Clark, J. *et al.* Fusion of splicing factor genes PSF and NonO (p54nrb) to the *TFE3* gene in papillary renal cell carcinoma. *Oncogene* **15**(18), 2233–2239 (1997).
- Argani, P. *et al.* A novel CLTC-*TFE3* gene fusion in pediatric renal adenocarcinoma with t(X;17)(p11.2;q23). *Oncogene* **22**(34), 5374–5378 (2003).
- Huang, W. *et al.* Identification of a novel PARP14-*TFE3* gene fusion from 10-year-old FFPE tissue by RNA-seq. *Genes Chromosomes Cancer* **54**(8), 500–505 (2015).
- Malouf, G. G. *et al.* Genomic heterogeneity of translocation renal cell carcinoma. *Clin. Cancer Res.* **19**(17), 4673–4684 (2013).
- Argani, P. *et al.* *TFE3*-fusion variant analysis defines specific clinicopathologic associations among Xp11 translocation cancers. *Am. J. Surg. Pathol.* **40**(6), 723–737 (2016).
- Argani, P. *et al.* RBM10-*TFE3* renal cell carcinoma: A potential diagnostic pitfall due to cryptic intrachromosomal Xp11.2 inversion resulting in false-negative *TFE3* FISH. *Am. J. Surg. Pathol.* **41**(5), 655–662 (2017).
- de Jong, B. *et al.* Cytogenetics of a renal adenocarcinoma in a 2-year-old child. *Cancer Genet. Cytogenet.* **21**(2), 165–169 (1986).
- Ross, H. & Argani, P. Xp11 translocation renal cell carcinoma. *Pathology* **42**(4), 369–373 (2010).
- Geller, J. I. *et al.* Translocation renal cell carcinoma: Lack of negative impact due to lymph node spread. *Cancer* **112**(7), 1607–1616 (2008).
- Cohen, H. T. & McGovern, F. J. Renal-cell carcinoma. *N. Engl. J. Med.* **353**(23), 2477–2490 (2005).
- Zhuang, W. *et al.* Gender difference analysis of Xp11.2 translocation renal cell carcinomas's attack rate: A meta-analysis and systematic review. *BMC Urol.* **20**(1), 130 (2020).
- Cheng, X. *et al.* Clinical characteristics of XP11.2 translocation/*TFE3* gene fusion renal cell carcinoma: A systematic review and meta-analysis of observational studies. *BMC Urol.* **16**(1), 40 (2016).
- Lipworth, L., Tarone, R. E. & McLaughlin, J. K. The epidemiology of renal cell carcinoma. *J. Urol.* **176**(6 Pt 1), 2353–2358 (2006).
- Gul, Z. G., Liaw, C. W., Mehrazin, R. Gender differences in incidence, diagnosis, treatments, and outcomes in clinically localized bladder and renal cancer. *Urology*. (2020).
- Mancini, M., Righetto, M. & Baggio, G. Gender-related approach to kidney cancer management: Moving forward. *Int. J. Mol. Sci.* **21**(9), 3378 (2020).
- Shi, Q. *et al.* Estradiol increases risk of topoisomerase II β -mediated DNA strand breaks to initiate Xp11.2 translocation renal cell carcinoma. *Cell Commun. Signal* **19**(1), 114 (2021).
- Liu, N. *et al.* Both SUMOylation and ubiquitination of *TFE3* fusion protein regulated by androgen receptor are the potential target in the therapy of Xp11.2 translocation renal cell carcinoma. *Clin. Transl. Med.* **12**(4), e797 (2022).
- Caldon, C. E. Estrogen signaling and the DNA damage response in hormone dependent breast cancers. *Front. Oncol.* **4**, 106 (2014).
- Rouleau, N. *et al.* Novel ATPase of SNF2-like protein family interacts with androgen receptor and modulates androgen-dependent transcription. *Mol. Biol. Cell* **13**(6), 2106–2119 (2002).
- Zhang, F. P. *et al.* An adenosine triphosphatase of the sucrose nonfermenting 2 family, androgen receptor-interacting protein 4, is essential for mouse embryonic development and cell proliferation. *Mol. Endocrinol.* **21**(6), 1430–1442 (2007).
- Sabirzhanov, B. *et al.* Irradiation-induced upregulation of miR-711 inhibits DNA repair and promotes neurodegeneration pathways. *Int. J. Mol. Sci.* **21**(15), 5239 (2020).
- Sun, L. *et al.* Impact of estrogen on the relationship between obesity and renal cell carcinoma risk in women. *EBioMedicine* **34**, 108–112 (2018).
- Wu, S. T. *et al.* Cellular effects induced by 17- β -estradiol to reduce the survival of renal cell carcinoma cells. *J. Biomed. Sci.* **23**(1), 67 (2016).
- Scully, R. *et al.* DNA double-strand break repair-pathway choice in somatic mammalian cells. *Nat. Rev. Mol. Cell Biol.* **20**(11), 698–714 (2019).

29. Domanskyi, A. *et al.* Expression and localization of androgen receptor-interacting protein-4 in the testis. *Am. J. Physiol. Endocrinol. Metab.* **292**(2), E513–E522 (2007).
30. Olde, B. & Leeb-Lundberg, L. M. GPR30/GPER1: Searching for a role in estrogen physiology. *Trends Endocrinol. Metab.* **20**(8), 409–416 (2009).
31. Guo, X. *et al.* Estrogen receptor α regulates ATM expression through miRNAs in breast cancer. *Clin. Cancer Res.* **19**(18), 4994–5002 (2013).
32. Wada-Hiraike, O. *et al.* The DNA mismatch repair gene hMSH2 is a potent coactivator of oestrogen receptor α . *Br. J. Cancer* **92**(12), 2286–2291 (2005).
33. Dunford, A. *et al.* Tumor-suppressor genes that escape from X-inactivation contribute to cancer sex bias. *Nat. Genet.* **49**(1), 10–16 (2017).
34. Sultan, I. *et al.* Comparing children and adults with synovial sarcoma in the Surveillance, Epidemiology, and End Results program, 1983 to 2005: An analysis of 1268 patients. *Cancer* **115**(15), 3537–3547 (2009).
35. Hagerty, B. L. *et al.* Characterization of alveolar soft part sarcoma using a large national database. *Surgery* **168**(5), 825–830 (2020).
36. Rais-Bahrami, S. *et al.* Xp11 translocation renal cell carcinoma: Delayed but massive and lethal metastases of a chemotherapy-associated secondary malignancy. *Urology* **70**(1), 178.e3–6 (2007).
37. Al-Mashaikhi, N. *et al.* Renal cell carcinoma with Xp 11.2 translocation as a second tumor in a long-term survivor of advanced neuroblastoma. *Pediatr. Hematol. Oncol.* **32**(3), 215–222 (2015).
38. Song, W. *et al.* Targeting newly identified ER β /TGF- β 1/SMAD3 signals with the FDA-approved anti-estrogen Faslodex or an ER β selective antagonist in renal cell carcinoma. *Mol. Oncol.* **12**(12), 2055–2071 (2018).
39. Fucic, A. *et al.* Environmental exposure to xenoestrogens and oestrogen related cancers: Reproductive system, breast, lung, kidney, pancreas, and brain. *Environ. Health* **11**(Suppl 1), S8 (2012).
40. Guan, B. Z. *et al.* Activation of G protein coupled estrogen receptor (GPER) promotes the migration of renal cell carcinoma via the PI3K/AKT/MMP-9 signals. *Cell Adh. Migr.* **12**(2), 109–117 (2018).
41. Li, J. J. & Li, S. A. Estrogen carcinogenesis in Syrian hamster tissues: Role of metabolism. *Fed. Proc.* **46**(5), 1858–1863 (1987).
42. Epstein, R. J. & Smith, P. J. Estrogen-induced potentiation of DNA damage and cytotoxicity in human breast cancer cells treated with topoisomerase II-interactive antitumor drugs. *Cancer Res.* **48**(2), 297–303 (1988).
43. Sasanuma, H. *et al.* BRCA1 ensures genome integrity by eliminating estrogen-induced pathological topoisomerase II-DNA complexes. *Proc. Natl. Acad. Sci. U. S. A.* **115**(45), E10642–e10651 (2018).
44. Tsuchiya, Y., Nakajima, M. & Yokoi, T. Cytochrome P450-mediated metabolism of estrogens and its regulation in human. *Cancer Lett.* **227**(2), 115–124 (2005).
45. Newbold, R. R. & Liehr, J. G. Induction of uterine adenocarcinoma in CD-1 mice by catechol estrogens. *Cancer Res.* **60**(2), 235–237 (2000).
46. Nebert, D. W. Elevated estrogen 16 α -hydroxylase activity: Is this a genotoxic or nongenotoxic biomarker in human breast cancer risk? *J. Natl. Cancer Inst.* **85**(23), 1888–1891 (1993).
47. Rich, S. *et al.* Primary pulmonary hypertension. A national prospective study. *Ann. Intern. Med.* **107**(2), 216–223 (1987).
48. Austin, E. D. *et al.* Alterations in oestrogen metabolism: Implications for higher penetrance of familial pulmonary arterial hypertension in females. *Eur. Respir. J.* **34**(5), 1093–1099 (2009).
49. Mair, K. M. *et al.* Obesity alters oestrogen metabolism and contributes to pulmonary arterial hypertension. *Eur. Respir. J.* **53**(6), 1801524 (2019).
50. Liu, C. *et al.* Ultraviolet A light induces DNA damage and estrogen-DNA adducts in Fuchs endothelial corneal dystrophy causing females to be more affected. *Proc. Natl. Acad. Sci. U. S. A.* **117**(1), 573–583 (2020).
51. Stapelfeld, C., Dammann, C. & Maser, E. Sex-specificity in lung cancer risk. *Int. J. Cancer* **146**(9), 2376–2382 (2020).

Acknowledgements

This work was supported by Medical Research Project of Jiangsu Commission of Health (ZD2022013) and Nanjing SCI-TECH Development Project (201803025), Beijing Ronghe Medical Development Foundation and Jiangsu Provincial Research and Practice Innovation Program Project. The funders had no role in study design, data collection and analysis, decision to publish, or preparation of the manuscript. The authors thank (Nuclear Medicine Department of Nanjing Drum Tower Hospital) for offering estrogen data.

Author contributions

Conception and design: Y.L. and W.G.; administrative support: W.G., D.L. and H.G.; provision of study materials or patients: W.M., F.Y. and X.D.; collection and assembly of data: Y.L., Y.Z. and N.L.; data analysis and interpretation: Y.L. and Q.S.; manuscript writing: all authors; final approval of manuscript: all authors.

Competing interests

The authors declare no competing interests.

Additional information

Supplementary Information The online version contains supplementary material available at <https://doi.org/10.1038/s41598-023-33363-0>.

Correspondence and requests for materials should be addressed to W.G.

Reprints and permissions information is available at www.nature.com/reprints.

Publisher's note Springer Nature remains neutral with regard to jurisdictional claims in published maps and institutional affiliations.



Open Access This article is licensed under a Creative Commons Attribution 4.0 International License, which permits use, sharing, adaptation, distribution and reproduction in any medium or format, as long as you give appropriate credit to the original author(s) and the source, provide a link to the Creative Commons licence, and indicate if changes were made. The images or other third party material in this article are included in the article's Creative Commons licence, unless indicated otherwise in a credit line to the material. If material is not included in the article's Creative Commons licence and your intended use is not permitted by statutory regulation or exceeds the permitted use, you will need to obtain permission directly from the copyright holder. To view a copy of this licence, visit <http://creativecommons.org/licenses/by/4.0/>.

© The Author(s) 2023